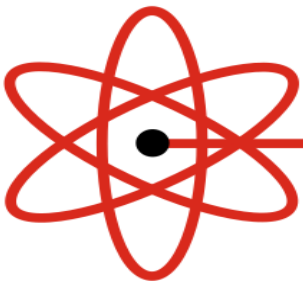




Competitiveness Operational Programme (COP)
Extreme Light Infrastructure - Nuclear Physics
(ELI-NP) – Phase II



Nuclear Photonics 2025
October 6 - 10, 2025 in Darmstadt, Germany



What can we learn from studying
PDR and GDR with microscopic
theory including phonon coupling

N. Tsoneva



Motivation

The Theoretical Model

- Phenomenological EDF approach extended with three-phonon QPM theory.

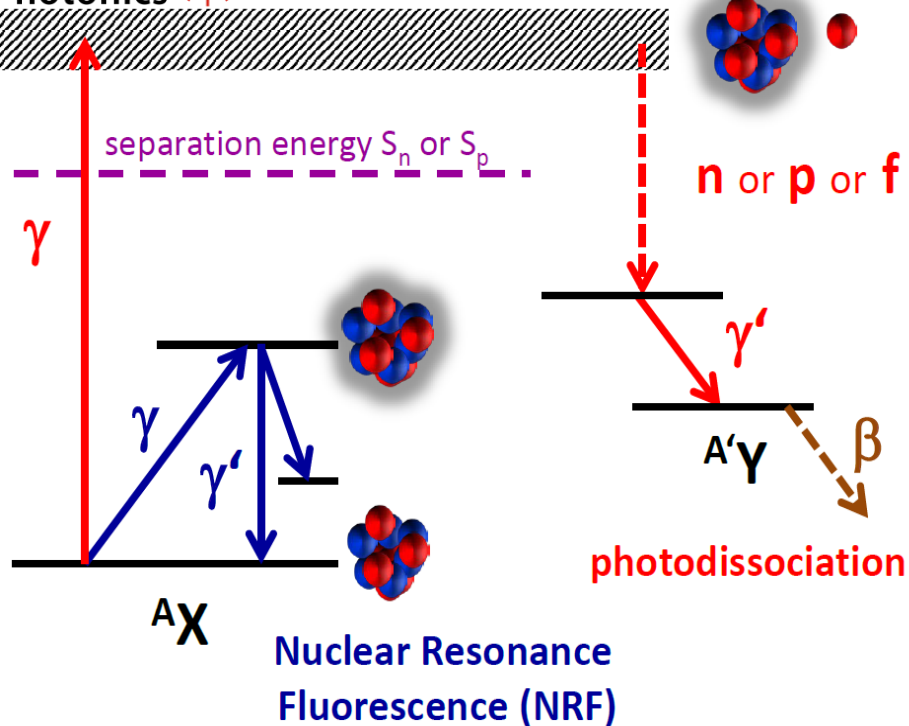
Nuclear response on external EM and hadronic fields

- Two-phonon states, pygmy and giant resonances: Are the pygmy resonances related to the access of neutrons in nuclei?
- Spectroscopic properties of the PDR derived with different probes and techniques. Multi-configuration mixing and branching ratios. Fine structure of PDR.
- First study of the γ -strength functions in $^{112,114}\text{Sn}$ by using the Oslo method at ELI-NP&IFIN-HH. EQPM interpretation of the experimental data.
- γ -decay of GDR in ^{112}Sn .
- Testing the role of the quasicontinuum below the neutron threshold: (γ, γ') vs. (p, p') .

Conclusions and Outlook

Nuclear Structure Studies with Photonuclear Reactions

Nuclear Photonics



Quasimonoeenergetic, highly polarized γ beams at the High-Intensity γ -Ray Source (**HI γ S**) operated by the Triangle Universities Nuclear Laboratory (**TUNL**) in Durham, North Carolina, USA.

The γ -beam system at ELI-NP (under construction)

NRF experiments will play a special role at the ELI-NP facility involving detailed high-resolution studies of the dipole strength distribution in the region of the PDR and giant dipole resonances GDR.

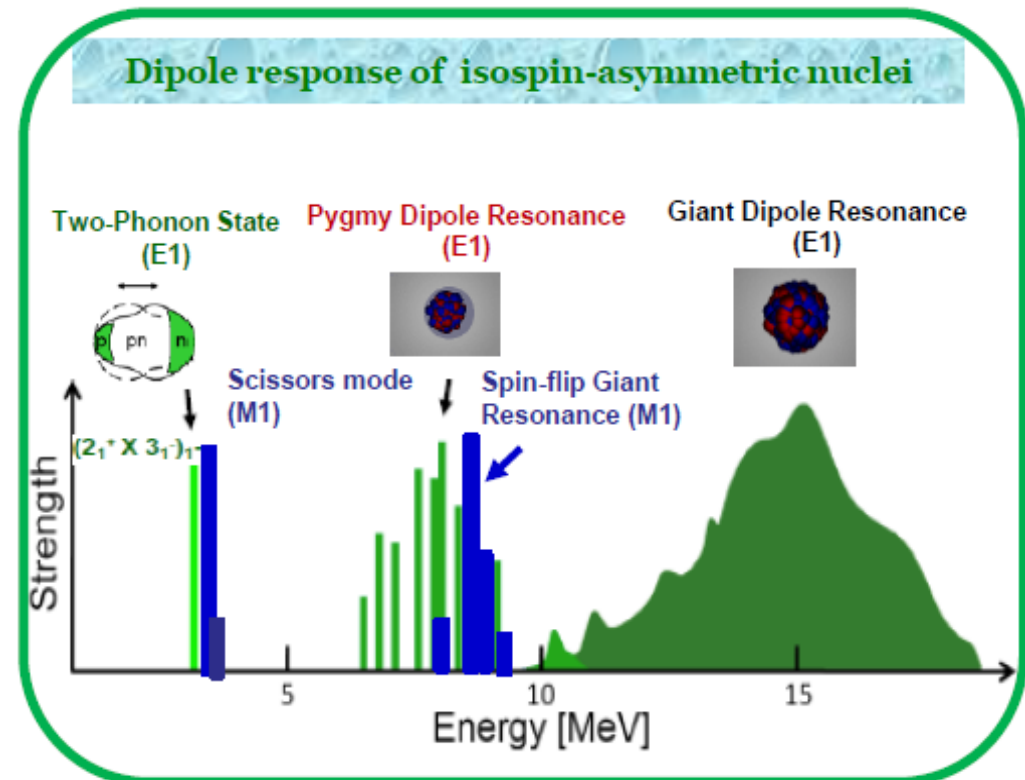
- Two-Phonon 1⁻ Excitation: $B(E1) \sim 10^{-3}$ W.u.
- Pygmy Dipole Resonance: $B(E1) \sim 0.5$ W.u.
- Giant Dipole Resonance: $B(E1) \sim 5 - 12$ W.u.

GDR: M.N. Harakeh, A. van der Woude, Giant Resonances, Oxford University Press (2001).

PDR: D. Savran, T. Aumann, A. Zilges, PNP 70, 210 (2013).

A. Bracco, F.C.L. Crespi, E.G. Lanza, EPJA 51, 99 (2015).

QOS: U. Kneissl, N. Pietralla, and A. Zilges, J. Phys. G32, R217 (2006).



The QPM Hamiltonian:

$$H = \boxed{H_{MF}} + \boxed{H_{res}}$$

HFB

$$H_{res} = H_M^{ph} + H_{SM}^{ph} + H_M^{pp}$$

$$H = \sum_{\lambda\mu i} \omega_{\lambda i} Q_{\lambda\mu i}^+ Q_{\lambda\mu i} + \frac{1}{2} \sum_{\lambda_1\lambda_2\lambda_3 i_1 i_2 i_3 \mu_1 \mu_2 \mu_3} C_{\lambda_1\mu_1\lambda_2\mu_2}^{\lambda_3-\mu_3} \times U_{\lambda_1 i_1}^{\lambda_2 i_2}(\lambda_3 i_3) [Q_{\lambda_1\mu_1 i_1}^+ Q_{\lambda_2\mu_2 i_2}^+ Q_{\lambda_3-\mu_3 i_3} + h.c.],$$

The QPM basis is built of phonons:

$$Q_{\lambda\mu i}^+ = \frac{1}{2} \sum_{j_1 j_2} \left[\psi_{j_1 j_2}^{\lambda i} A_{\lambda\mu}^+(j_1, j_2) - (-1)^{\lambda-\mu} \varphi_{j_1 j_2}^{\lambda i} A_{\lambda-\mu}(j_1, j_2) \right]$$

$$A_{\lambda\mu}^+(j_1, j_2) = \sum_{m_1 m_2} \langle j_1 m_1 j_2 m_2 | \lambda \mu \rangle \alpha_{j_1 m_1}^+ \alpha_{j_2 m_2}^+$$

$$A_{\lambda-\mu}(j_1, j_2) = \sum_{m_1 m_2} \langle j_1 m_1 j_2 m_2 | \lambda - \mu \rangle \alpha_{j_2 m_2} \alpha_{j_1 m_1}$$

The phonons are not 'pure' bosons:

$$[Q_{\lambda\mu i}, Q_{\lambda'\mu' i'}^+] = \delta_{\lambda\lambda'} \delta_{\mu\mu'} \delta_{ii'} + \text{fermionic corrections} \\ \sim \alpha_{j_1 m_1}^+ \alpha_{j_2 m_2}$$

QRPA equations are solved:

$$[H, Q_{\lambda\mu i}^+] = E_{\lambda\mu i} Q_{\lambda\mu i}^+$$

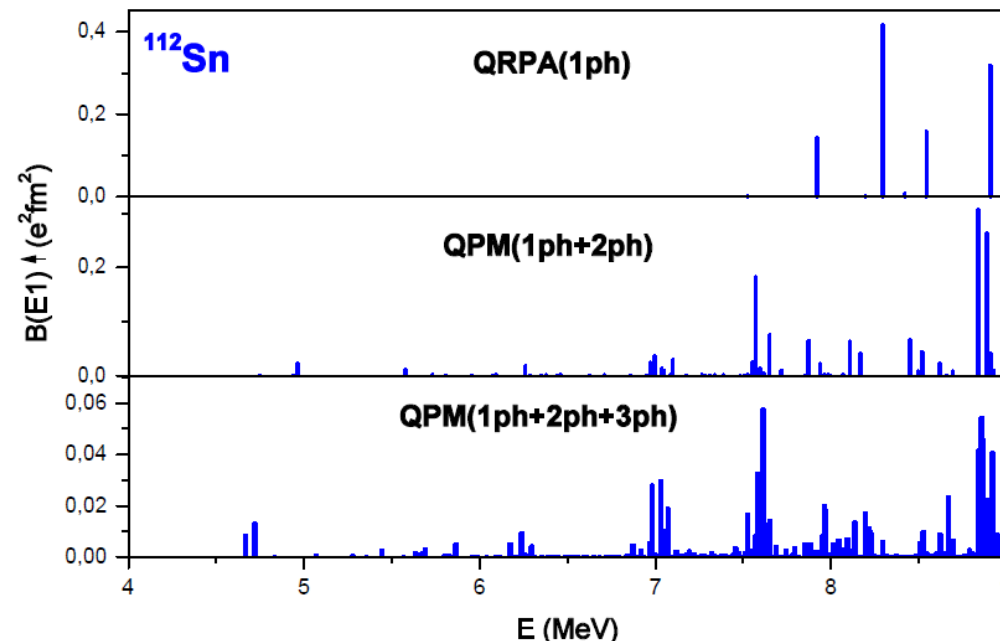
Multi-Configuration Multi-Quasiparticle Wave Function

$$|\Psi\rangle = \sum_{abc} \left[X_a + X_{ab} + X_{abc} \right]$$

$$\Psi_\nu(JM) = \left\{ \sum_i R_i(J\nu) Q_{JM_i}^+ + \sum_{\substack{\lambda_1 i_1 \\ \lambda_2 i_2}} P_{\lambda_2 i_2}^{\lambda_1 i_1}(J\nu) [Q_{\lambda_1 \mu_1 i_1}^+ \otimes Q_{\lambda_2 \mu_2 i_2}^+]_{JM} \right. \quad (1)$$

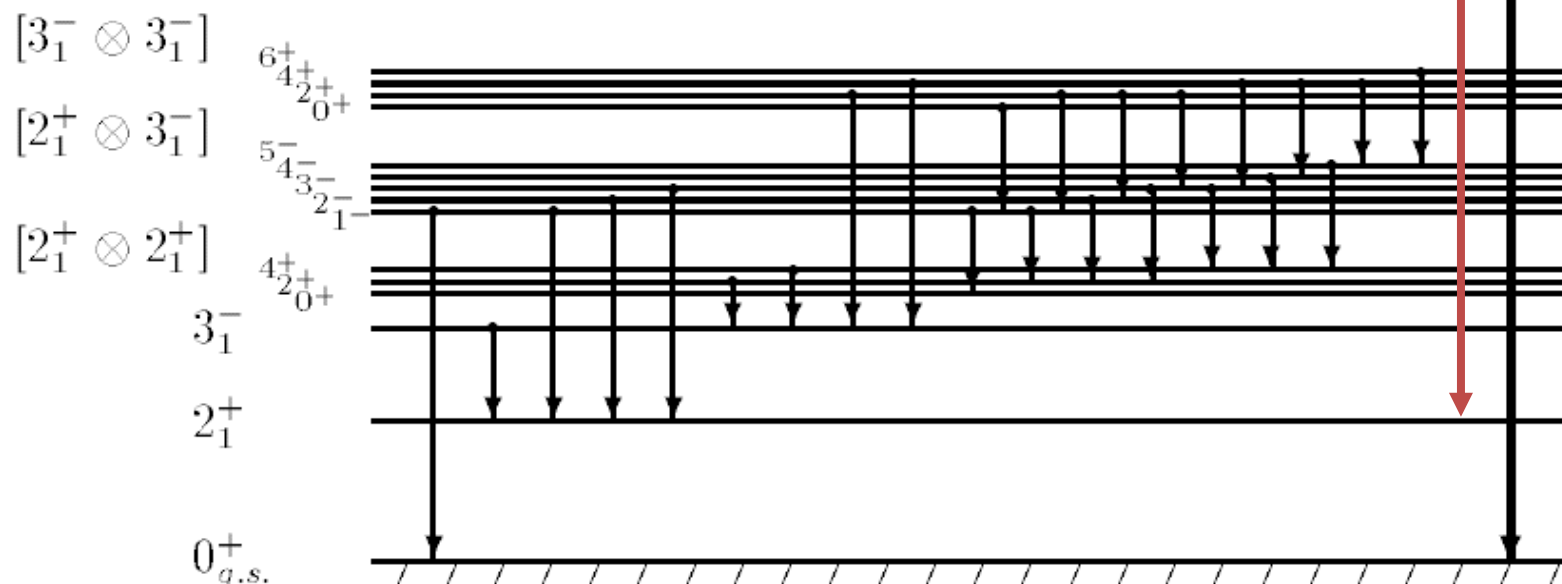
$$\left. + \sum_{\substack{\lambda_1 i_1 \lambda_2 i_2 \\ \lambda_3 i_3}} T_{\lambda_3 i_3}^{\lambda_1 i_1 \lambda_2 i_2 I}(J\nu) [[Q_{\lambda_1 \mu_1 i_1}^+ \otimes Q_{\lambda_2 \mu_2 i_2}^+]_{IK} \otimes Q_{\lambda_3 \mu_3 i_3}^+]_{JM} \right\} \Psi_0 \quad (2)$$

- Basis of QRPA phonons
- „ph“ and „pp“- type configurations
- Pauli principle, orthogonality
- Core polarization effects
- Large multi-particle-multi-hole configuration space
- **SPECTRAL FRAGMENTATION**
- **SPECTRAL SHIFTS**



GDR

? What is the nature of the GDR



$$M(X\lambda) = \langle \Psi_f || T(X\lambda) || \Psi_i \rangle$$

$$T(X\lambda) = T^{Ph}(X\lambda) + T^{QPh}(X\lambda)$$

QRPA $\sim Q^+_{\lambda\mu}$

QPM $\sim \alpha^+_{jm} \alpha_{j'm'}$

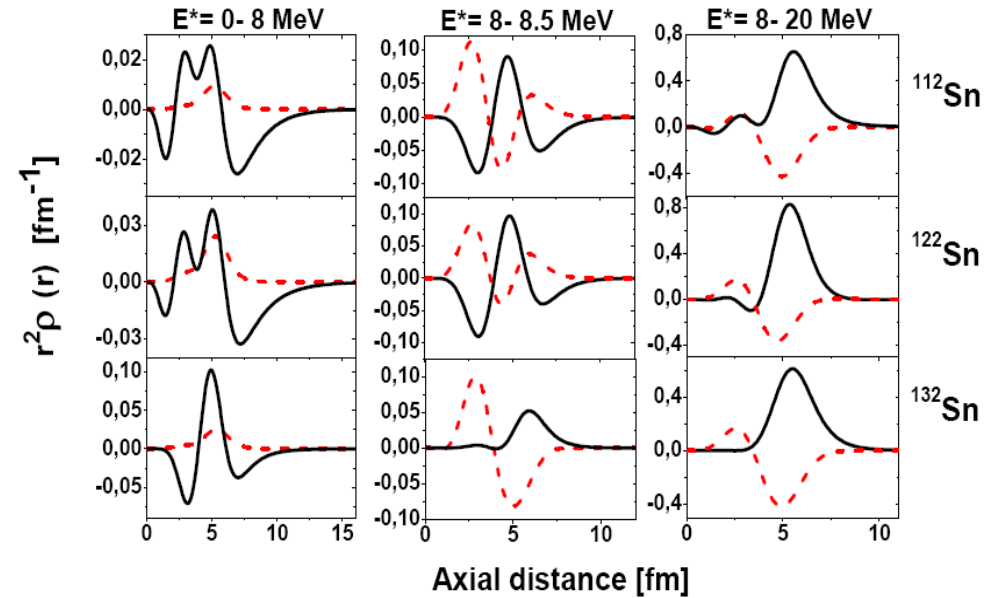
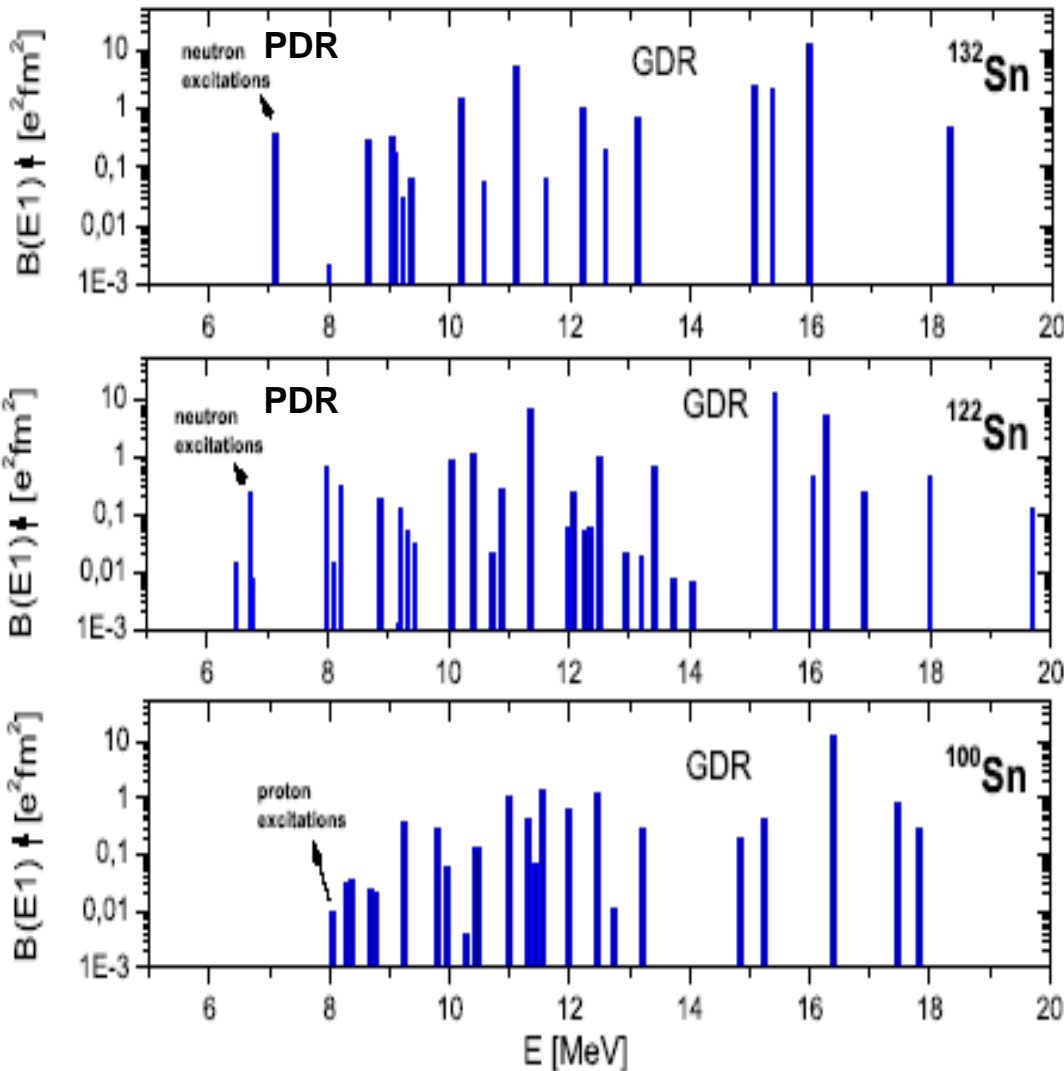
J. Kleemann, N. Pietralla et al., PRL134 022503 (2025)
Gamma-decay of the IVGDR in ^{154}Sm

QRPA calculations on the dipole response in Sn Isotopes

N. Tsoneva, H. Lenske, Ch. Stoyanov, Phys. Lett. B 586, 213 (2004)

H. Lenske, N. Tsoneva, Eur. Phys. J. A (2019) 55: 238 (2019)

N. Tsoneva, H. Lenske, PRC 77, 024321 (2008)



Relation between the non-energy weighted dipole sum rule and the skin measure

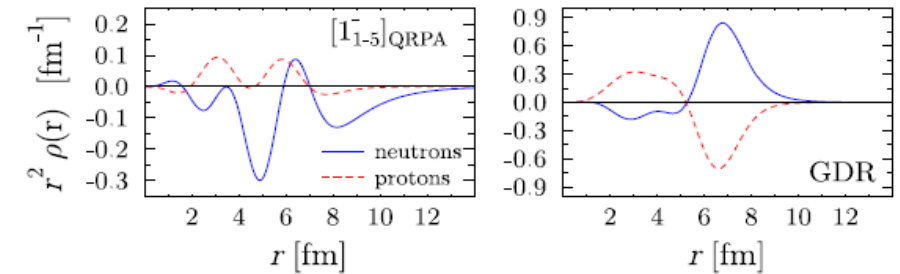
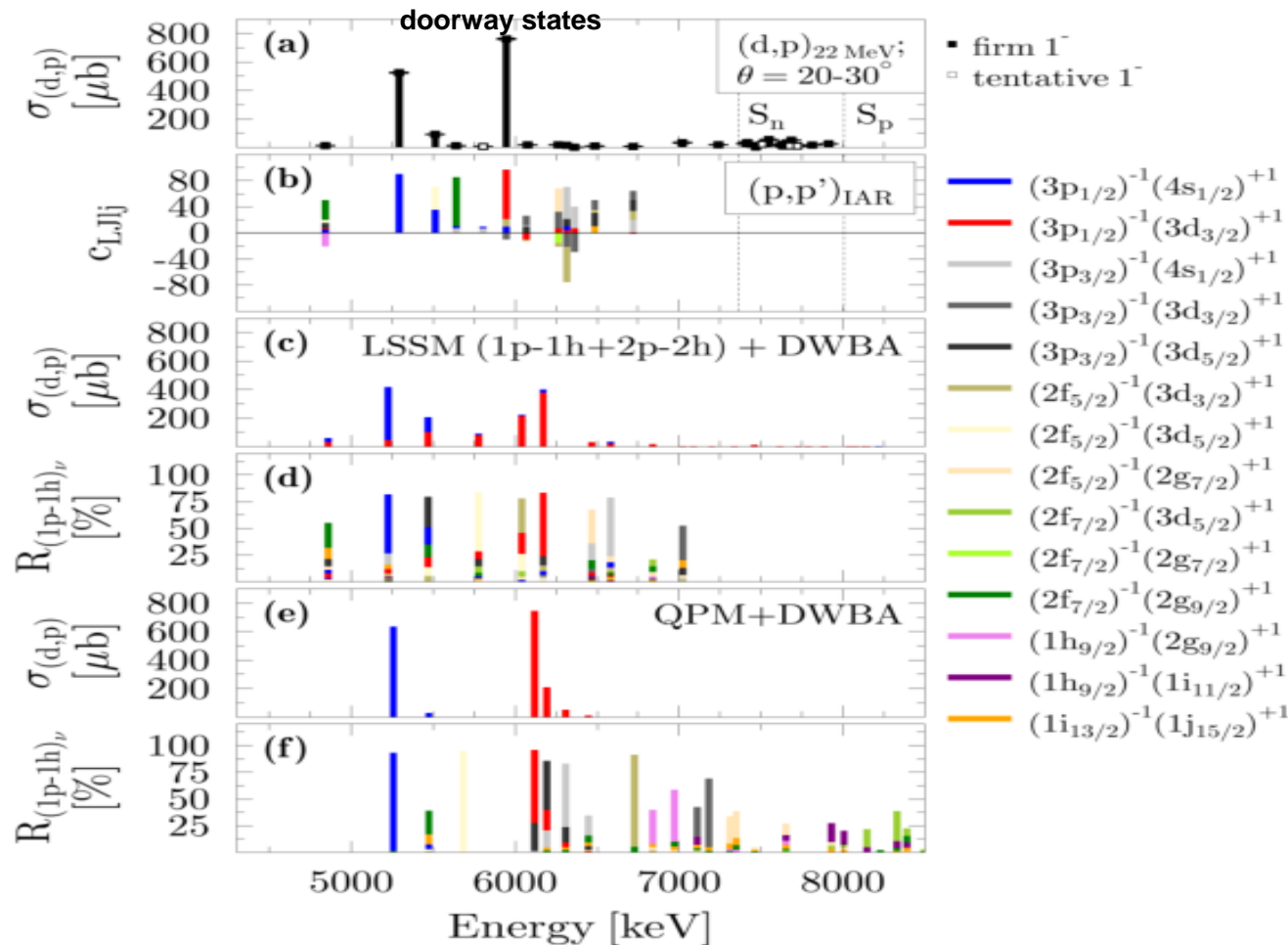
$$\Delta_3 r^2 = \frac{1}{4q_0 q_1} \left(\sum_d B_d(E1) - q_0^2 \sum_d |M_d^{(0)}|^2 - q_1^2 \sum_d |M_d^{(1)}|^2 \right)$$

Accessing the Single-Particle Structure of the Pygmy Dipole Resonance in ^{208}Pb

M. Spieker, A. Heusler, B. A. Brown, T. Faestermann, R. Hertenberger, G. Potel, M. Scheck, N. Tsoneva, M. Weinert, H.-F. Wirth, and A. Zilges, *Phys. Rev. Lett.* **125**, 102503 (2020)



Unprecedented access to the theoretical wave functions demonstrating the 1p-1h neutron origin of the PDR in ^{208}Pb



[B.A. Brown (LSSM) and N. Tsoneva (QPM)]

Below S_n :

$$\sum \sigma_{(d,p);\text{exp.}} = 1524(17) \mu\text{b}$$

$$\sum \sigma_{(d,p);\text{LSSM}} = 1470 \mu\text{b}$$

$$\sum \sigma_{(d,p);\text{QPM}} = 1676 \mu\text{b}$$



Above S_n and up to S_p :

$$\sum \sigma_{(d,p);\text{exp.}} = 254(9) \mu\text{b}$$

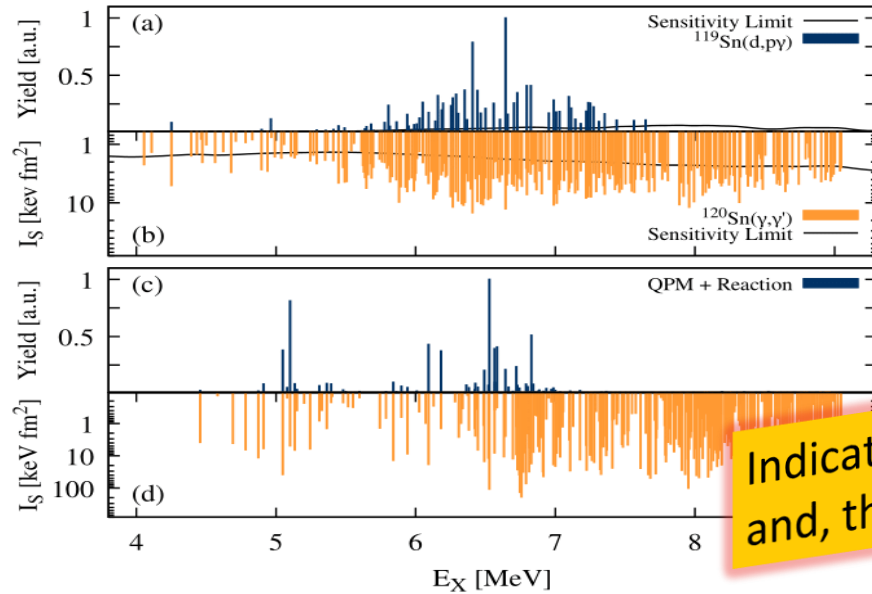
$$\sum \sigma_{(d,p);\text{LSSM}} = 22 \mu\text{b}$$



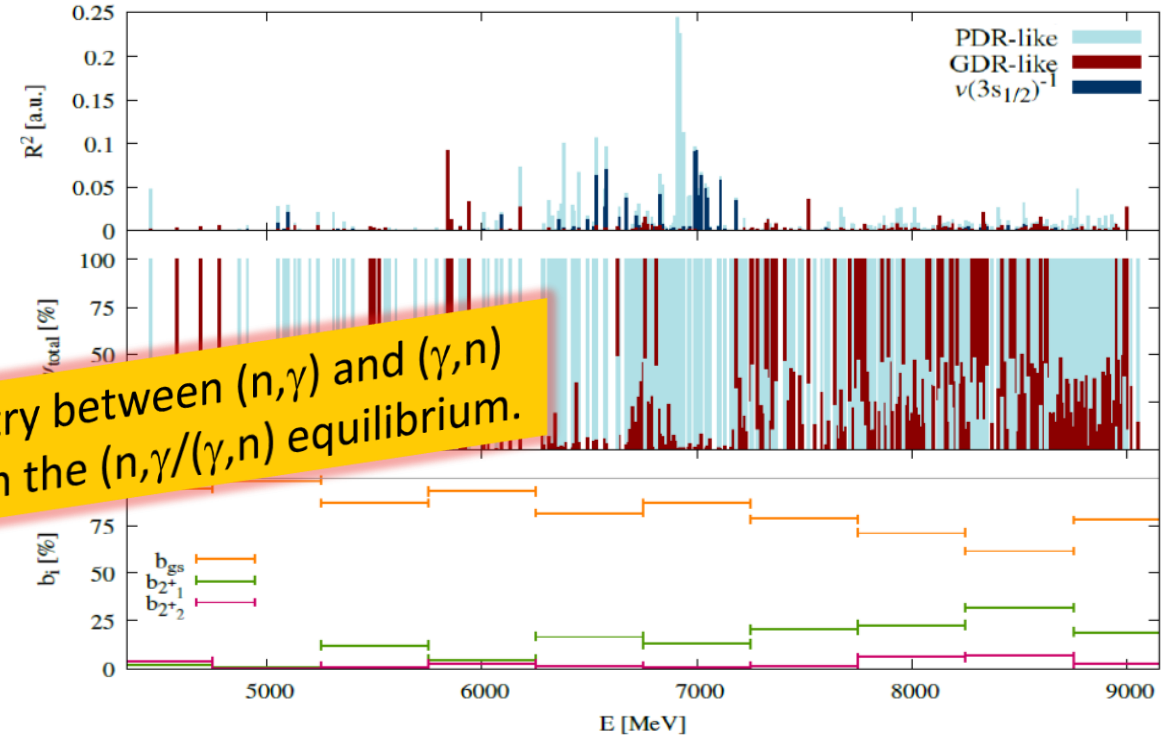
Single-Particle Structure of the Pygmy Dipole Resonance in ^{120}Sn

M. Weinert, M. Spieker, G. Potel, N. Tsoneva, M. Müscher, J. Wilhelmy and A. Zilges, PRL 127, 242501 (2021)

EDF+QPM+reaction theory



Indication of asymmetry between (n,γ) and (γ,n) and, thus, influence on the $(n,\gamma)/(\gamma,n)$ equilibrium.



$$\frac{d\sigma_{\nu}}{d\Omega}(\theta) = \frac{\mu_i \mu_f}{(2\pi\hbar^2)^2} \frac{k_f}{k_i} \times \left| u_{3p_{1/2}} R_{3p_{1/2}}(\nu) \psi_{\frac{1}{2} \frac{1}{2}}^{3p_{1/2}} \mathcal{T}_{p_{1/2}}(\theta) + u_{3p_{3/2}} R_{3p_{3/2}}(\nu) \psi_{\frac{1}{2} \frac{3}{2}}^{3p_{3/2}} \mathcal{T}_{p_{3/2}}(\theta) \right|^2$$

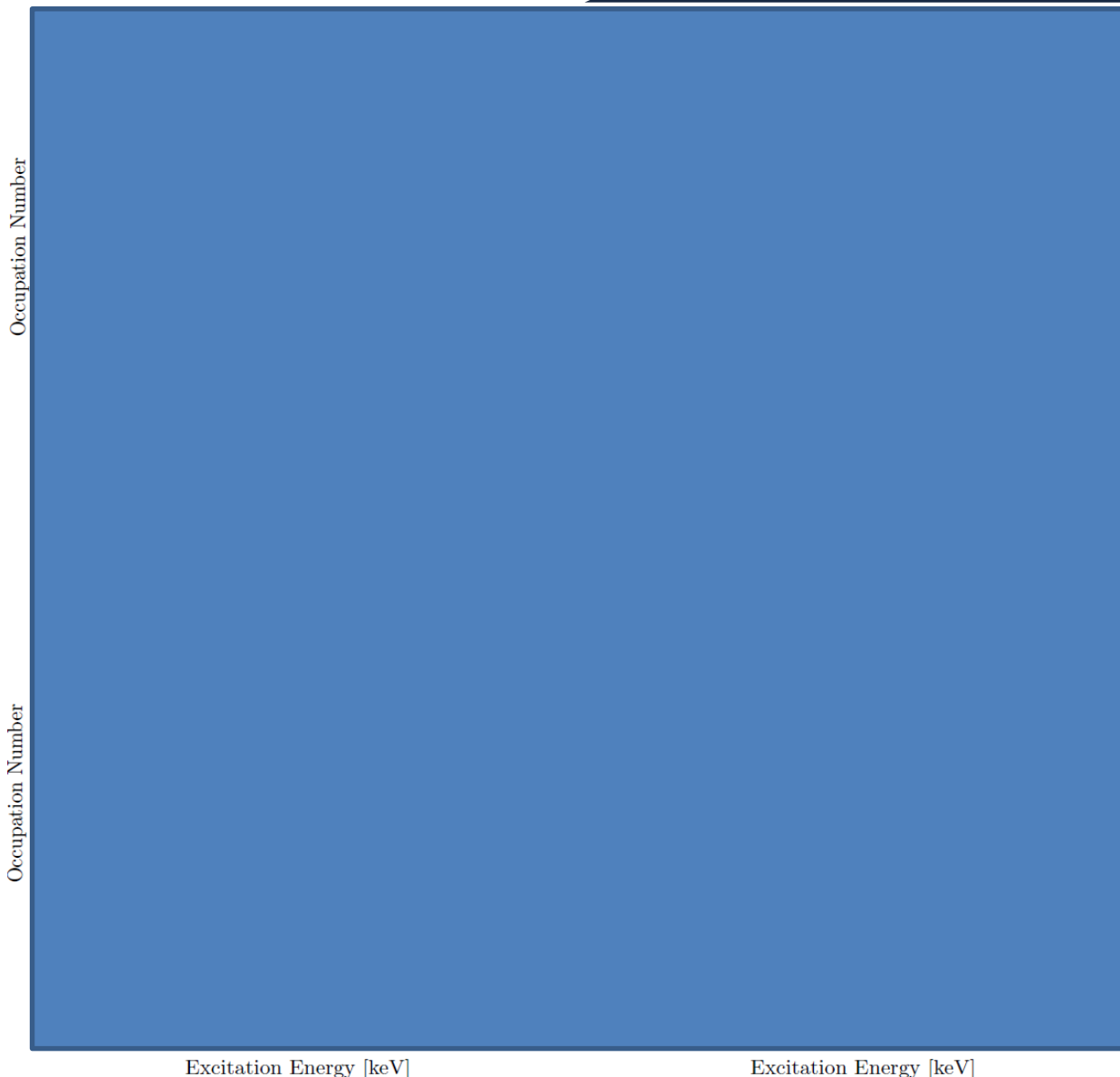
E_{cm} for $3p_{3/2}$ and $3p_{1/2}$: $E_{\text{cm}}^{\text{exp}} = 6.49$ MeV;
 $E_{\text{cm}}^{\text{QPM}} = 6.32$ MeV.

Summed energy-integrated cross section:

NRF data: $\sum I_s^{\text{NRF}} = 337(21)$ keV, (d,py) yield $>1\%$

$\sum I_s^{\text{QPM}} = 243 - 360$ keV fm² for 1^- states with
 (d,py) yield $>1\%$ and $>0.5\%$.

Comprehensive study of the electric and magnetic dipole strength in semi-magic ^{50}Ti



The study combines data from single-neutron transfer (d, p) obtained at the FSU John D. Fox Laboratory and real-photon scattering experiments from TU Darmstadt, and the HIGS facility of TUNL, which allowed us to map out the B(E1) and B(M1) strength fragmentation up to the neutron-separation energy, and to gain access to associated spectroscopic factors determined in (d,p). The experimental results are compared with three-phonon EQPM incl. configuration space with $J^\pi=1^{+,-}6^{+,-}$

A detailed view at magnetic dipole strengths: The case of semi-magic ^{50}Ti

B. Kelly, U. Friman-Gayer, M. Spieker, L.T. Baby, A.L. Conley, J. Isaak, E. Litvinova, H. Pai, N. Pietralla, N. Tsoneva, A. Volya, and V. Werner, in preparation for submission.

Investigating the microscopic structure of the PDR near the N =50 region,

T. C. Khumalo, L. Pellegri, A. Spatafora, D. Carbone, M. Cavallaro, F. Cappuzzello, N. Tsoneva, et al., in preparation.

$^{97}\text{Mo}(p,d)^{96}\text{Mo}$ and $^{95}\text{Mo}(d,p)^{96}\text{Mo}$ transfer reactions were carried out using the MAGNEX magnetic spectrometer at INFN-LNS to test the PDR and its relationship to neutron skin oscillations. Extracted from measurements, model-dependent spectroscopic factors are compared with the three-phonon (EQPM) ones, in preparation for submission.

Study of the γ -strength function in $^{112,114}\text{Sn}$ at ELI-NP&IFIN-HH

Total EDF+QPM dipole strength below the neutron separation threshold S_n :

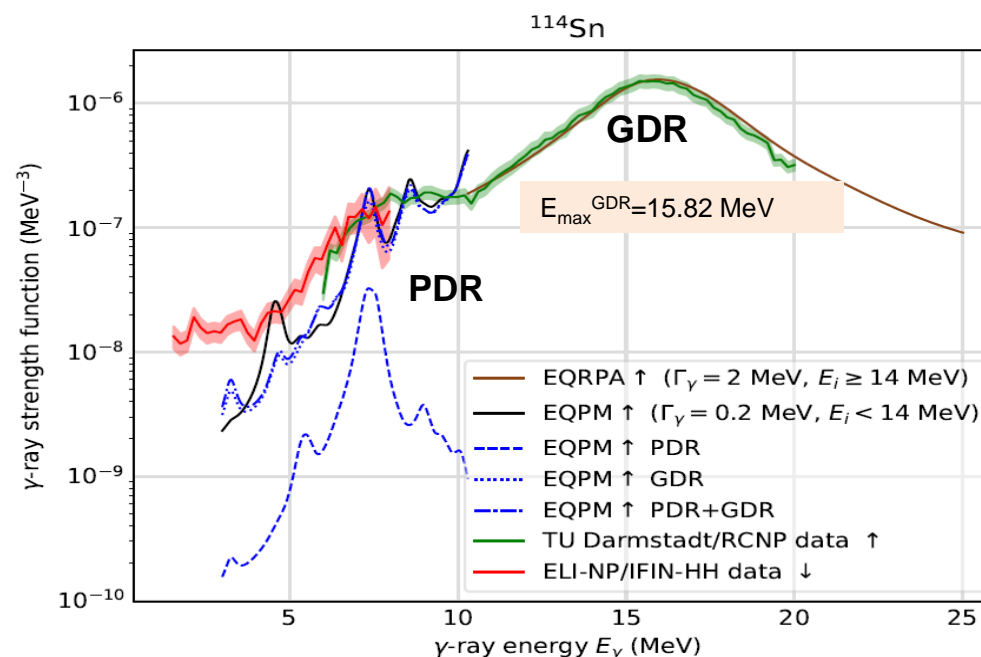
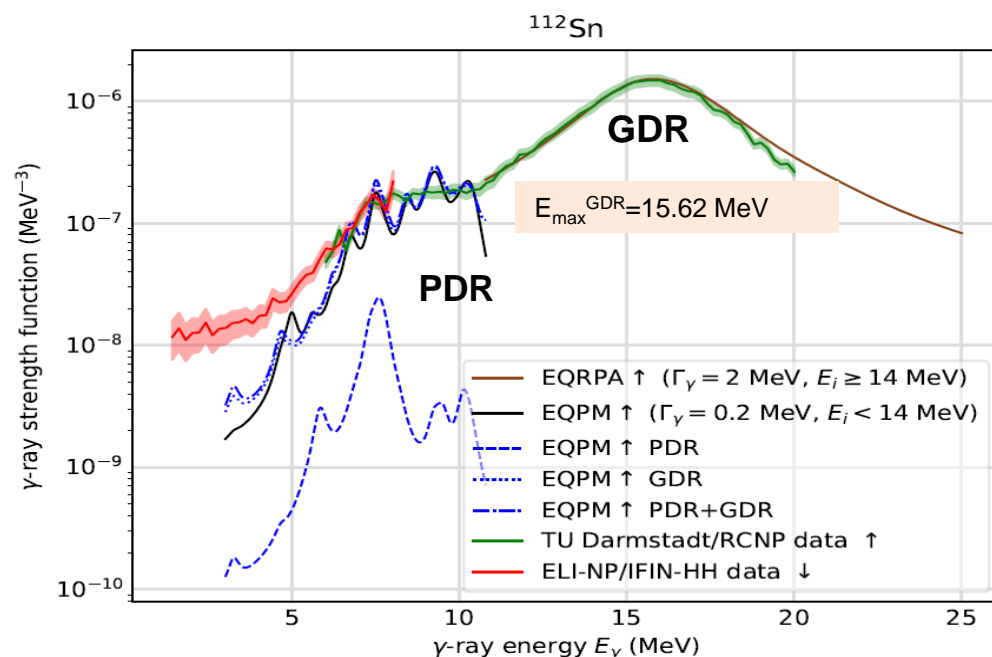
$\sigma_{\text{EQPM}}(E_1)E_n = 127.3 \text{ mb}\cdot\text{MeV}$ in ^{112}Sn and $S_n \sigma_{\text{EQPM}}(E_1)E_n = 107.3 \text{ mb}\cdot\text{MeV}$ in ^{114}Sn ,

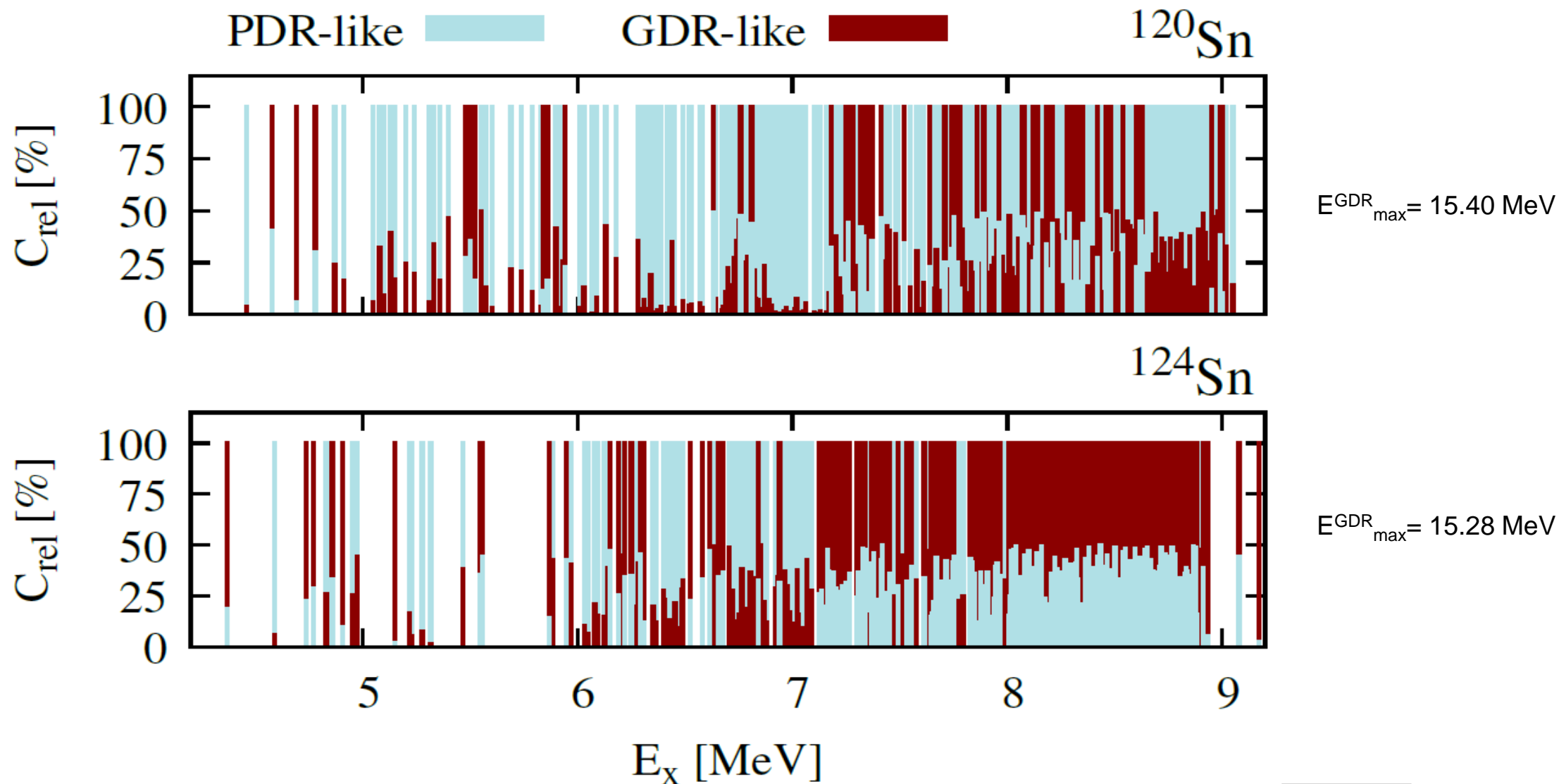
Experimental strength, below S_n :

$\sigma_{\text{exp}}(E_1)E_n = 110(8) \text{ mb}\cdot\text{MeV}$ (^{112}Sn) and $\sigma_{\text{exp}}(E_1)E_n = 91(8) \text{ mb}\cdot\text{MeV}$ in ^{112}Sn

From the calculation of the integrated pure PDR peak from the EQPM, we see that the total PDR strength increases with increasing neutron number, from **4.38 mb·MeV** (^{112}Sn) (0.26% of the TRK EWSR) to **4.70 mb·MeV** (^{114}Sn) (0.28% of the TRK EWSR), as expected, while the total low-energy dipole strength is decreasing due to the admixture of more complex configurations and the GDR.

PDR strength increases with N number!



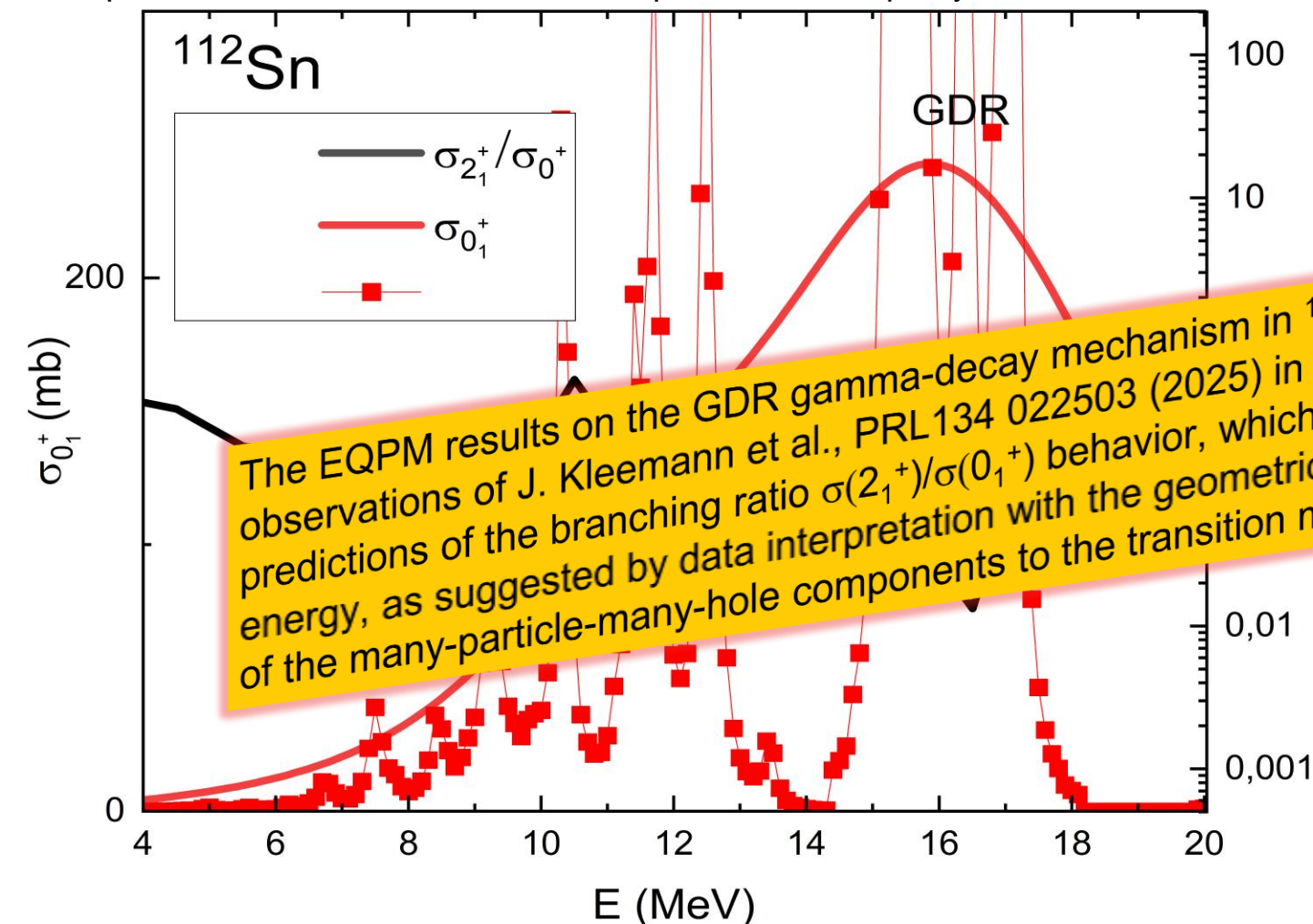


EQPM studies of the PDR and GDR decay properties

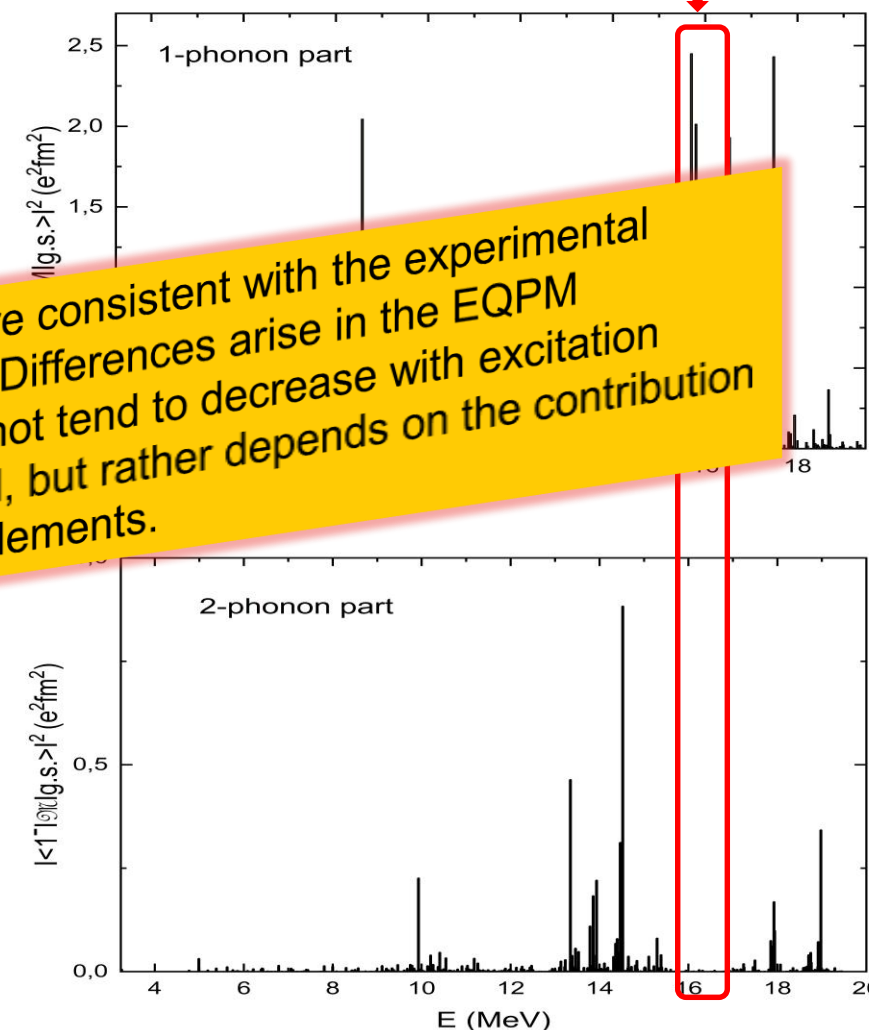
N. Tsoneva, in preparation

2-phonon EQPM calculations, model space of natural parity states with J=1-4

γ -decay of the GDR through
1ph 1^- collective states



The EQPM results on the GDR gamma-decay mechanism in ^{112}Sn are consistent with the experimental observations of J. Kleemann et al., PRL 134 022503 (2025) in ^{154}Sm . Differences arise in the EQPM predictions of the branching ratio $\sigma(2_1^+)/\sigma(0_1^+)$ behavior, which does not tend to decrease with excitation energy, as suggested by data interpretation with the geometric model, but rather depends on the contribution of the many-particle-many-hole components to the transition matrix elements.



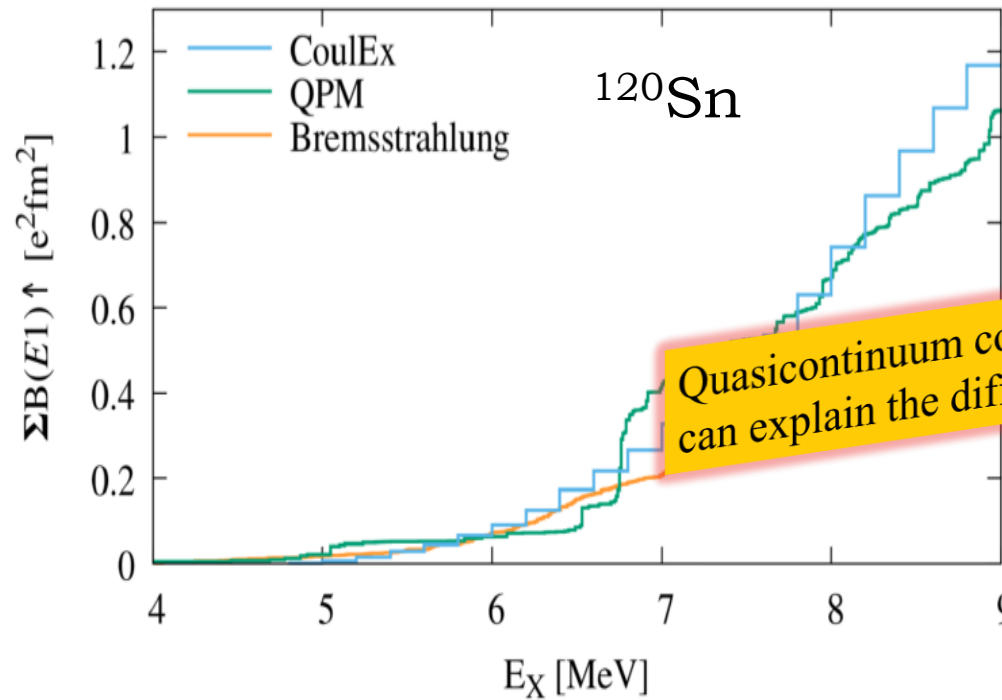
Electric dipole photoabsorption: (γ, γ') vs. (p, p')

M. Mscher et al., PRC 102, 014317 (2020)

N. Tsoneva, A. Ramirez, A. Tonchev, J. Silano, R. Schwengner et al., in preparation

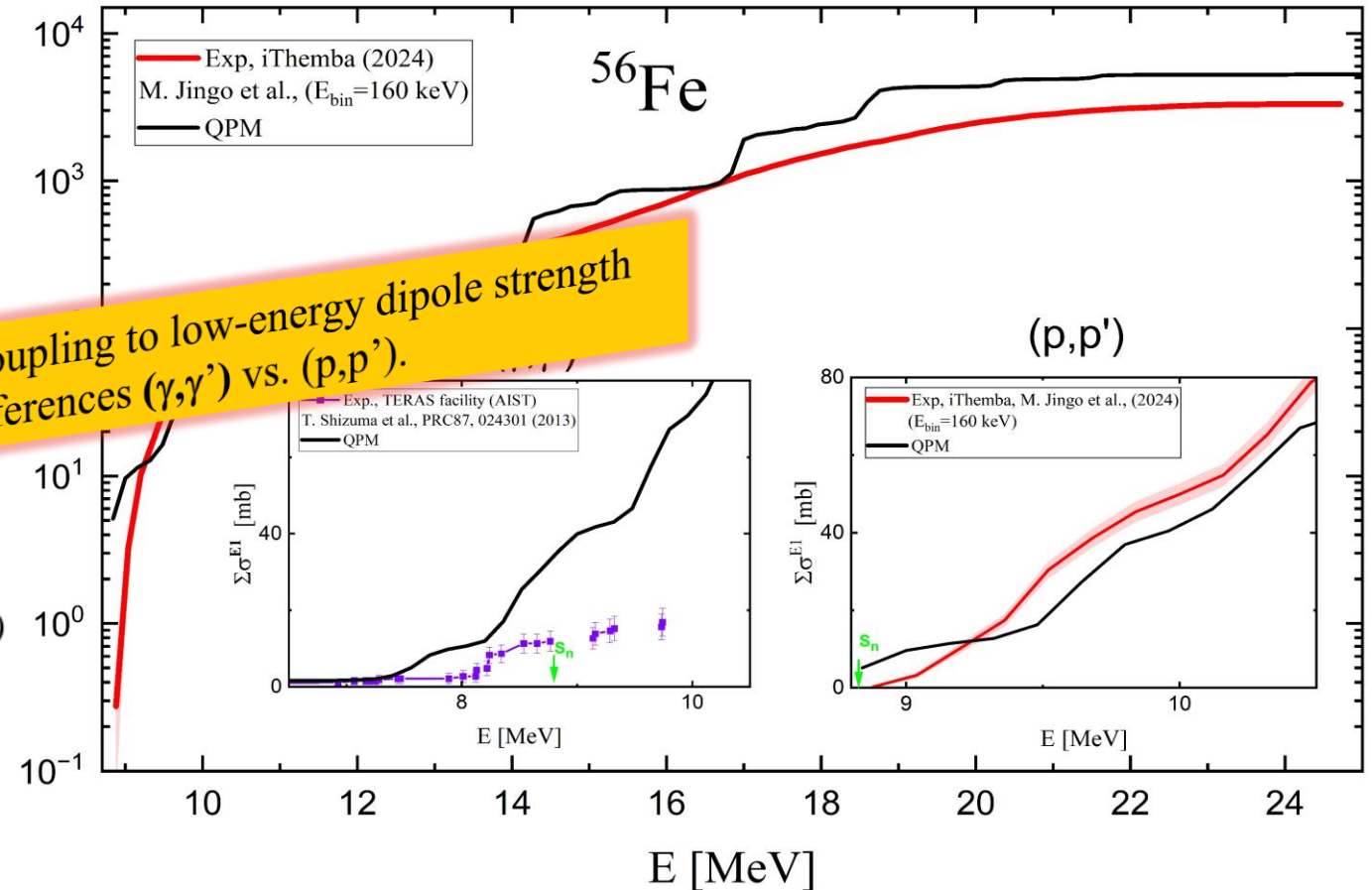
M. Weinert, M. Spieker, G. Potel, N. Tsoneva, M. Mscher, J. Wilhelmy and A. Zilges, PRL 127, 242501 (2021)

$B(E1) \uparrow$ running sums from (γ, γ') and (p, p') -CoulEx



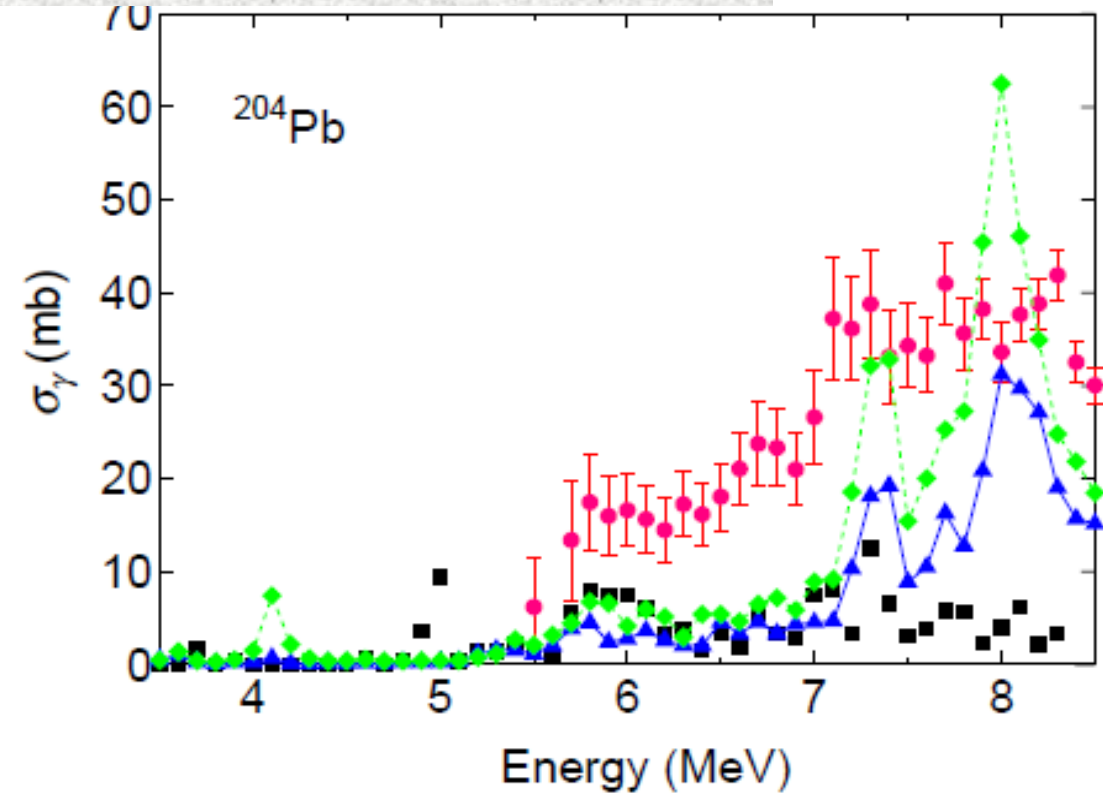
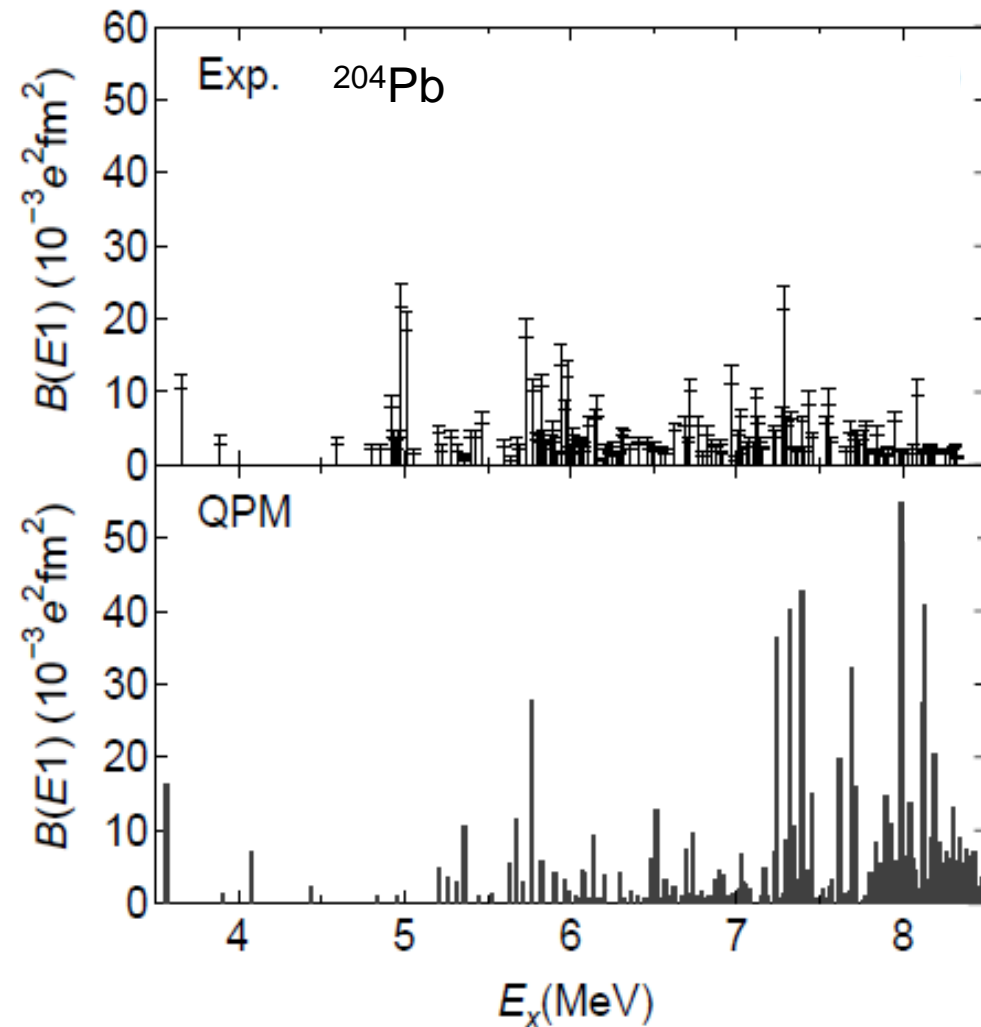
QPM reproduces CoulEx data nicely!

Quasicontinuum coupling to low-energy dipole strength can explain the differences (γ, γ') vs. (p, p') .



Contribution of the quasicontinuum to the low-lying dipole strength in ^{204}Pb

T. Shizuma, S. Endo, A. Kimura, R. Massarczyk, R. Schwengner, R. Beyer, T. Hensel, H. Hoffmann, A. Junghans, K. Römer, S. Turkat, A. Wagner, and N. Tsoneva, Phys. Rev. C 106, 044326 (2022)



Exp.: γ -ray absorption cross sections derived from resolved peaks (squares) and from the quasicontinuum analysis (red circles), averaged over energy bins of 100 keV;

EDF+ 3-phonon QPM confined in the NRF energy domain (blue triangles) and extended **EDF+2-phonon QPM** (green diamonds) calculations, smeared by the Lorentzian width of 100 keV.

A theoretical semi-microscopic approach based on EDF+QPM and nuclear reaction theory is applied in studies of nuclear structure properties and dynamics of nuclear excitations up to GDR energies:

- > enables a uniform description of multiphonon states, pygmy and giant resonances with the highest precision;
- > EQPM plus reaction theory studies of PDR - (γ, γ') vs. (d, p) : 1p-1h coherently excited neutron states, located in a confined energy region
- > Studies on PDR strength in ^{112}Sn and ^{114}Sn : total PDR strength follows the BSE sum rule; the PDR strength increases with excitation energy, the dipole strength below the neutron threshold depends on the coupling to the continuum
- > The two-phonon EQPM prediction for γ -decay in ^{112}Sn : through 1ph 1-collective states, with almost no contribution from 2ph components. The results do not support the concept of γ -decay of the isovector GDR through a compound nucleus.
- > Differences arise in the EQPM predictions and geometrical model interpretation of experimental data in ^{154}Sm of the branching ratio $\sigma(2_1^+)/\sigma(0_1^+)$, which does not tend to decrease with excitation energy, but rather depends on the contribution of the many-particle-many-hole components to the transition matrix elements.
- > Branching ratios to ground and excited \leftrightarrow multi-particle-multi-hole configuration mixing;
- > Quasicontinuum coupling to low-energy dipole strength can explain the differences (γ, γ') vs. (p, p') .

Thank you!